Cell, Vol. 103, 29–40, September 29, 2000, Copyright ©2000 by Cell Press

A Mechanism for Translationally Coupled mRNA Turnover: Interaction between the Poly(A) Tail and a c-*fos* RNA Coding Determinant via a Protein Complex

Christophe Grosset,*‖ Chyi-Ying A. Chen,*‖ Nianhua Xu,* Nahum Sonenberg,† Helene Jacquemin-Sablon,‡ and Ann-Bin Shyu*§

*Department of Biochemistry and Molecular Biology
The University of Texas Houston Medical School
Houston, Texas 77030
†Department of Biochemistry
McGill University
Montreal, Quebec
Canada H3G 1Y6
‡CNRS UPR 9044
Genetique Moleculaire et Integration des Fonctions Cellulaires
Institut de Recherches sur le Cancer
BP 8
94801 Villejuif
France

Summary

mRNA turnover mediated by the major protein-coding-region determinant of instability (mCRD) of the c-*fos* proto-oncogene transcript illustrates a functional interplay between mRNA turnover and translation. We show that the function of mCRD depends on its distance from the poly(A) tail. Five mCRD-associated proteins were identified: Unr, a purine-rich RNA binding protein; PABP, a poly(A) binding protein; PAIP-1, a poly(A) binding protein interacting protein; hnRNP D, an AU-rich element binding protein; and NSAP1, an hnRNP R-like protein. These proteins form a multiprotein complex. Overexpression of these proteins stabilized mCRD-containing mRNA by impeding deadenylation. We propose that a bridging complex forms between the poly(A) tail and the mCRD and ribosome transit disrupts or reorganizes the complex, leading to rapid RNA deadenylation and decay.

Introduction

The 3′ poly(A) tail, in association with poly(A) binding proteins (PABP), plays a critical role in eukaryotic mRNA metabolism (Manley and Proudfoot, 1994; Jacobson, 1996). In the process of cytoplasmic mRNA turnover, the poly(A) tail is thought to have a passive and protective role, and must be shortened to a minimal length prior to decay of the transcribed portion of the transcript. Although it has been shown that various known mammalian RNA destabilizing elements, e.g., AU-rich elements (Chen and Shyu, 1995) and protein-coding determinants (Ross, 1995), direct rapid removal of poly(A) tail as a necessary first step in mRNA decay, the underlying mechanisms and participating *trans*-acting factors remain largely unknown.

Recently, the poly(A) tail has been shown to stimulate both cap-dependent and cap-independent translation initiation in the cytoplasm (Gallie, 1991; Tarun et al., 1997; Preiss and Hentze, 1998). The observations that both the 5′ cap and 3′ poly(A) tail influence cap-dependent translation initiation and that avid protein/protein interactions occur among PABP, eIF4G, and eIF4E (the cap binding protein) suggest a physical interaction between the two mRNA termini, which enhances translation initiation (Sachs et al., 1997; Preiss and Hentze, 1999). Further evidence supporting such an interaction comes from the observation of circular mRNPs involving these protein interactions with the 5′ cap and 3′ poly(A) tail (Wells et al., 1998). These studies raised important questions as to whether the 3′ poly(A) tail communicates with other regions of an mRNA, such as RNA stability determinants and how such communication might be accomplished, thus influencing the fate of mRNA in the cytoplasm.

A large set of observations point to an important role for translation in the mRNA decay process. First, drugs or mutations that interfere with translation lead to mRNA stabilization (e.g., Schiavi et al., 1994; Yeilding et al., 1998). Second, some elements that dictate rapid mRNA decay are located within protein coding regions and their activity depends on ribosome translocation near the element (e.g., Yen et al., 1988; Shyu et al., 1989; Wisdom and Lee, 1991). Third, premature translational termination can enhance mRNA decay rates (for a recent review, see Hentze and Kulozik, 1999). Fourth, some degradative factors are polysome-associated (e.g., Caruccio and Ross, 1994; Zhang et al., 1997). Recent experiments using the c-*fos* mRNA as a model system have demonstrated a clear role for translation in mammalian RNA turnover (Schiavi et al., 1994). Two destabilizing regions within the c-*fos* protein coding region, termed CRD-1 and CRD-2, have been identified, and CRD-1 is the major determinant (mCRD) (Chen et al., 1992; Schiavi et al., 1994). Specifically inhibiting the translation of a reporter mRNA bearing either the entire c-*fos* protein coding region or just the mCRD by insertion of a stable stem-loop upstream of the translation initiation codon led to full stabilization of the message (Schiavi et al., 1994; Chen et al., 1995).

It has been shown that loss of poly(A) tail profoundly reduces the efficiency of translation initiation. Yet, the rapid decay directed by the mCRD requires ribosome transit, and deadenylation is a necessary first step coupled to translation (Shyu et al., 1991; Schiavi et al., 1994). Reconciling these seemingly contradictory observations in a model for mCRD-mediated RNA turnover has proven to be particularly challenging. Here, we report a critical finding that a minimal spacer sequence must be maintained between the c-*fos* mCRD and the poly(A) tail for the RNA destabilizing function of mCRD. This finding suggests communication between the mCRD and the poly(A) tail, perhaps via the formation of a unique "bridging" complex. In this interpretation, the 3′ poly(A)

§To whom correspondence should be addressed: (e-mail: ann-bin.shyu@uth.tmc.edu).

‖Both authors made equal contributions.

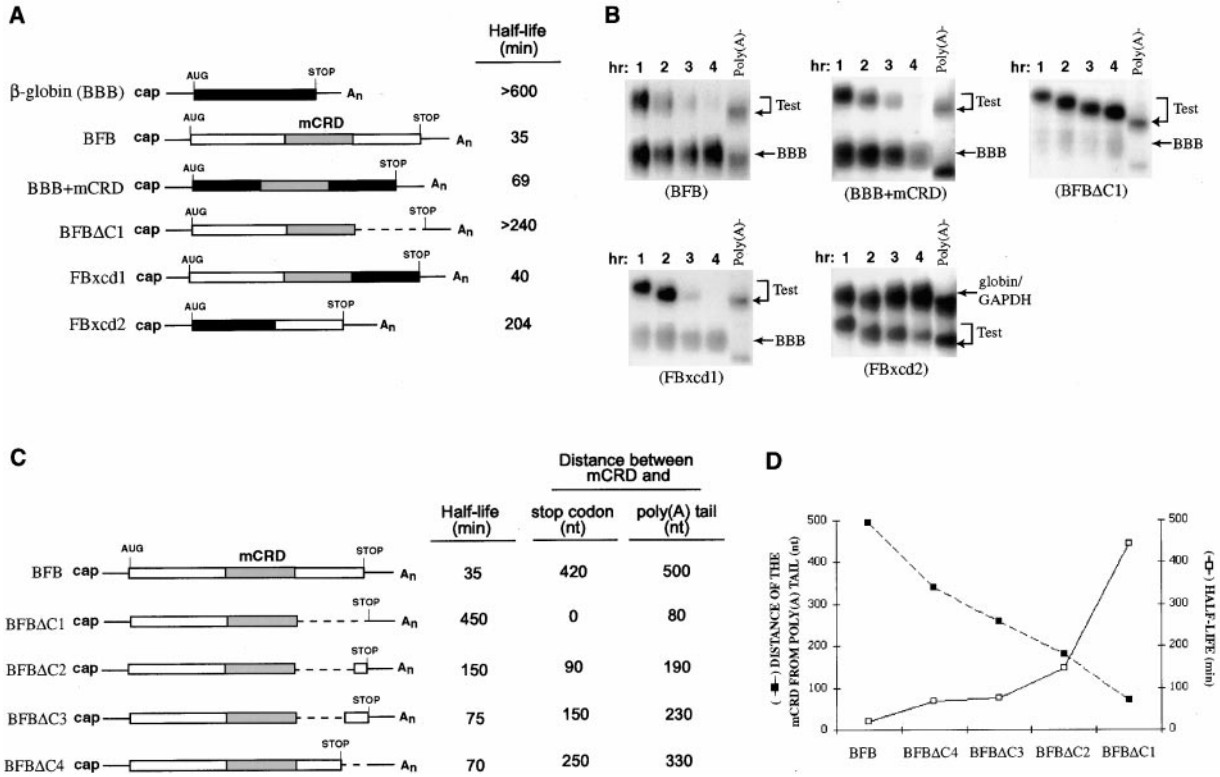

Figure 1. A Minimal Downstream Spacer Region Is Required for the Destabilizing Function of c-*fos* mCRD

(A) Physical maps and half-lives of β-globin mRNA (BBB) and the chimeric mRNAs derived from hybrids made between β-globin and c-*fos* coding regions. Solid lines: 5′ and 3′ UTRs from β-globin mRNA. Rectangles: protein-coding regions from β-globin (black) and c-*fos* (gray and open) mRNAs. The 320 nt c-*fos* mCRD is shown as a gray rectangle. Broken lines: regions deleted from the c-*fos* coding region.

(B) Northern blots showing deadenylation and decay of the chimeric mRNAs. To determine RNA half-life, NIH 3T3 cells were transiently cotransfected with a control plasmid (pSVB10 or pSVα/GAPDH) and one of the test plasmids as indicated. Total cytoplasmic mRNA was isolated from NIH 3T3 cells at various time intervals after serum stimulation of quiescent cells and analyzed by Northern blot analysis. Transcription of test constructs was driven by the serum-inducible c-*fos* promoter. BBB or globin/GAPDH control mRNAs were expressed constitutively and served as an internal standard. The times given at the top correspond to hours after serum stimulation. Poly(A)$^-$ RNA was prepared in vitro by treating RNA samples from the1 hr time point with oligo(dT) and RNase H.

(C) Physical maps, half-lives, and the distances between the c-*fos* mCRD and either the stop codon or the poly(A) tail of BFB mRNA and its deletion derivatives. The schematic drawings are as described in the legend to (A).

(D) Composite plot illustrating the relationship between the RNA destabilizing function of the c-*fos* mCRD and its physical distance from the 3′ poly(A) tail. The transient transfection of NIH 3T3 cells, RNA isolation, time course experiments, and RNA blot analysis are as described in the legend to (B).

is protected by the bridging complex against shortening before the message bearing the mCRD is translated. Following translation initiation and subsequent ribosome transit, this bridging complex is disrupted, leading to poly(A) removal and subsequent decay of the RNA body. In support of this model, we have used RNA-affinity chromatography to purify a group of proteins that associate specifically with the mCRD. We further showed that these proteins form a multiprotein complex. Our data provide insights into a mechanism by which RNA turnover is coupled to translation, and reveal an active role for the poly(A) tail in cytoplasmic mRNA turnover.

Results

Spacing between the c-*fos* mCRD and the poly(A) Tail Determines the RNA Destabilizing Function of the mCRD

All cytoplasmic mRNA decays described in this study were determined by carrying out time course experiments in NIH 3T3 cells using the transcriptional pulsing approach (Shyu et al., 1996). Because the mRNAs were transiently transcribed from the c-*fos* promoter following serum induction of quiescent NIH 3T3 cells, they were homogeneous in size. This made it possible to monitor poly(A) shortening as a function of time by Northern blot analysis (Chen et al., 1994).

Previously, we showed that a hybrid message (BFB), composed of the 5′ and 3′ UTRs from the stable β-globin mRNA and the protein-coding region from the labile c-*fos* mRNA, decays rapidly (Figures 1A and 1B; also see Shyu et al., 1991). Further swapping between the β-globin and c-*fos* transcripts identified a 320 nucleotide (nt) region located in the central portion of c-*fos* coding region as the major coding-region determinant of instability (mCRD, previously known as CRDI-1; Chen et al., 1992; Schiavi et al., 1994). The mCRD alone reduced the half-life of the β-globin mRNA from over 10 hr to ~1 hr when inserted in-frame into the β-globin coding region (Figures 1A and 1B, BBB+mCRD). Surprisingly, when the 450 nt c-*fos* coding sequence immediately

downstream of the mCRD was deleted from BFB transcript, the resulting mRNA decayed very slowly (Figures 1A and 1B, BFBΔC1). This suggested that either the 450 nt c-*fos* coding region downstream of mCRD contains a potent destabilizing element, or that sequence of the 450 nt region functions as a spacer required for the mCRD destabilizing function.

To test these possibilities, a 334 nt sequence corresponding to the C-terminal coding region of the β-globin mRNA was inserted in-frame and immediately downstream of the mCRD in BFBΔC1 to create FBxcd1 (Figures 1A and 1B). The FBxcd1 mRNA decayed as rapidly as the BFB message, showing that an irrelevant coding sequence was able to substitute for the 450 nt C-terminal coding sequence of c-*fos* to restore the destabilizing ability of mCRD. To further substantiate this result, the C terminus of β-globin coding region was replaced with the 450 bp C-terminal region of c-*fos*. The resulting message (Figures 1A and 1B, FBxcd2) exhibited little decay, indicating lack of destabilizing function in this region. The mCRD thus requires a downstream coding sequence for its destabilizing function, and this downstream sequence appears to function simply as a spacer.

To determine the minimal size of downstream spacer required for the mCRD destabilizing function, three individual in-frame deletions were made in the BFB gene to shorten the C-terminal 450 bp coding region of c-*fos* to 250, 150, and 90 bp, creating respective BFBΔC4, BFBΔC3, and BFBΔC2 constructs (Figures 1C and 1D). The results (Figures 1C and 1D) showed that the half-life of the mRNA was inversely proportional to the length of coding sequence downstream of the mCRD. The notion was further confirmed by the following experiments. The 334 bp C-terminal coding region of β-globin was deleted from the BBB+mCRD construct to create the BBB+mCRDΔC gene (Figure 2A). The result showed that BBB+mCRDΔC transcript no longer decayed fast. When the deleted region was replaced with the 450 nt c-*fos* C-terminal coding sequence, the resulting message decayed with the same half-life as that of BBB+mCRD (Figure 2, FBxcd3). These results demonstrated that the mCRD retained the property of downstream-spacer dependent destabilizing function when present in a heterologous context of β-globin mRNA.

Shortening the coding region downstream of mCRD reduces not only the distance between mCRD and the stop codon, but also the distance between the mCRD and 3′ poly(A). Therefore, we investigated which of these distances was critical. We reasoned that if the distance from the mCRD to the poly(A) tail, but not to the stop codon, is important, converting the 450 nt c-*fos* C-terminal coding region present in the FBxcd3 message (Figure 2A) into an untranslated segment should not change the lability of the message. Thus, a translation stop codon was introduced immediately downstream of the mCRD in the coding region of the FBxcd3 construct. The resulting message had the same lability as the FBxcd3, indicating that the distance between mCRD and the poly(A) tail is critical (Figure 2, FBxcd4). To further substantiate this result, the antisense of the 450 nt c-*fos* C-terminal region was inserted into the 3′ UTR of the BBB+mCRDΔC message (Figure 2A) to restore the distance between the mCRD and the poly(A) tail without changing the distance between mCRD and translation stop codon. The resulting transcript (Figure 3, FBxcd5)

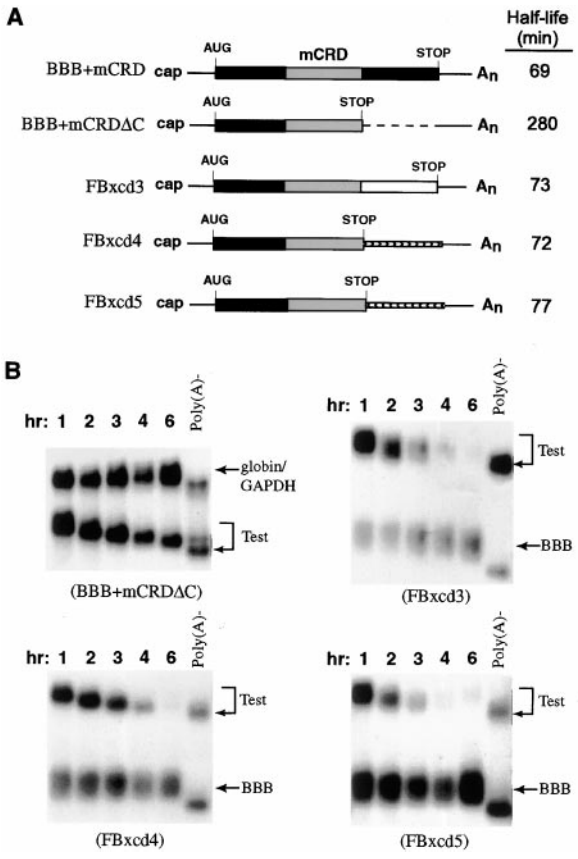

Figure 2. Spacing between the c-*fos* mCRD and the poly(A) Tail Is Required for the Destabilizing Function of the c-*fos* mCRD

(A) Physical maps and half-lives of BBB+mCRD mRNA and its derivatives. The schematic drawings are as described in the legend to Figure 1 except that the broken lines represent the regions deleted from the β-globin coding region, and that thin rectangles filled with arrowheads (rightward arrowheads: sense sequence; leftward arrowheads: antisense sequence) represent 3′ UTR sequences derived from the carboxyl terminal portion of the c-*fos* coding region.

(B) Northern blots showing the deadenylation and decay of BBB+mCRD and its derivative mRNAs. The transient transfection of NIH 3T3 cells, RNA isolation, time course experiments, and RNA blot analysis are as described in the legend to Figure 1.

decayed as rapidly as both the FBxcd3 and FBxcd4 mRNAs. Taken together, these results (Figures 1C, 1D, and 2) demonstrated that a minimal spacer of ~230 nt between the mCRD and the poly(A) tail is required for the 320 nt mCRD to exert its destabilizing function.

Mapping of the Minimal Functional Element in the c-*fos* mCRD

As part of an effort to identify and purify participating protein factors, we set out to map the minimal functional element within the mCRD. Previously, we showed that deleting either the 5′ 87 nt region or its immediate downstream 223 nt region from the mCRD rendered the mCRD nonfunctional (Chen et al., 1992). As shown in Figure 3, when the 87 nt region alone was inserted in-frame into the coding region of β-globin mRNA, the resulting message, BBB+cd87, was as stable as the wild-type β-globin mRNA. However, knowing the requirement for a minimal distance between the mCRD and the poly(A) tail,

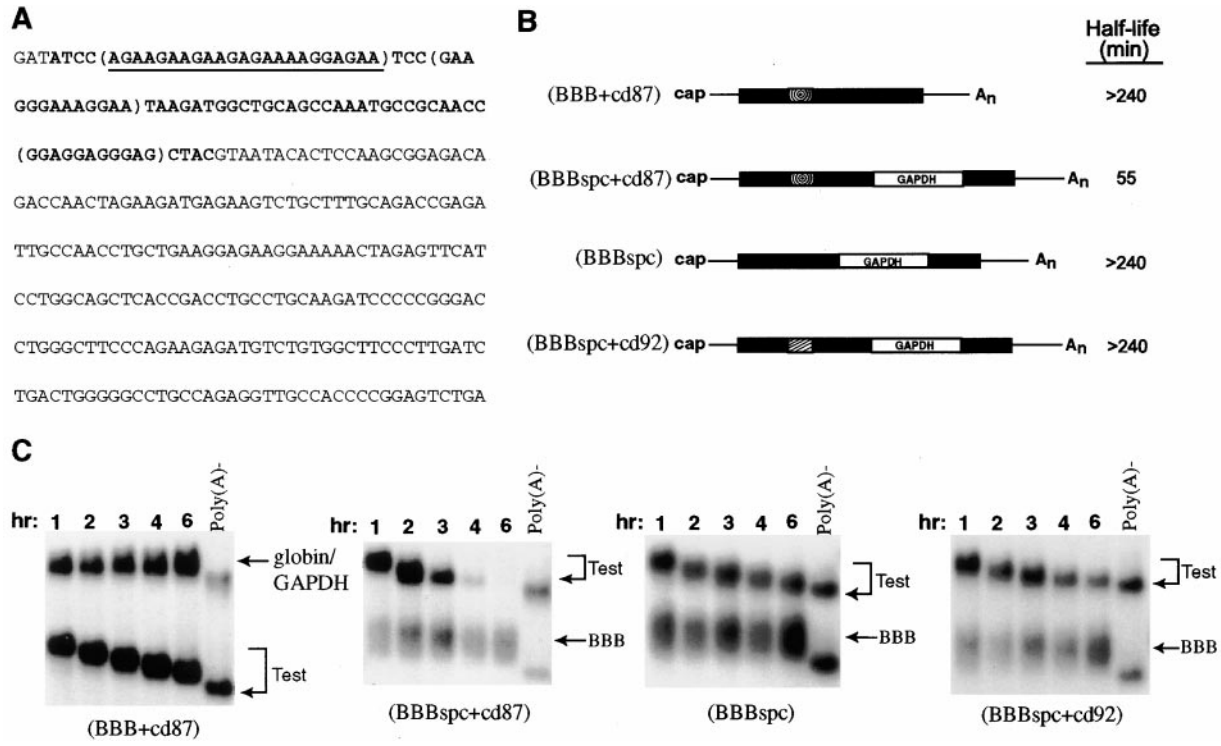

Figure 3. The Minimal Functional Element in the c-*fos* mCRD Is Mapped to Its 5′ 87 nt Purine-Rich Sequence

(A) RNA sequence of the 320 nt human c-*fos* mCRD. The 5′ 87 nt purine-rich sequence of the c-*fos* mCRD (the minimal functional element) is indicated by boldface characters, three purine stretches are in parentheses, and the 24 nt purine sequence used for protein purification is underlined.

(B) Physical maps and half-lives of BBB+cd87, BBBspc+cd87, BBBspc and BBBspc+cd92 mRNAs. Radial box: the 87 nt minimal functional element. Solid lines: 5′ and 3′ UTRs from β-globin mRNA. Solid rectangle: protein-coding region from β-globin. Hatched box: a 92 nt sequence form the 3′ portion of the c-*fos* mCRD (sequence in panel A). A 314 nt protein coding sequence from the rat *GAPDH* is indicated as an open box marked GAPDH and is referred to as "spc" in the names for chimeric mRNAs.

(C) Northern blots showing the deadenylation and decay of BBB+cd87, BBBspc+cd87, BBBspc, and BBBspc+cd92 mRNAs. The transient transfection of NIH 3T3 cells, RNA isolation, time course experiments, and RNA blot analysis are as described in the legend to Figure 1.

we tested whether the 223 nt sequence downstream of the 87 nt region simply served as spacer and thus could be replaced by an irrelevant sequence. When a 314 nt coding sequence from the rat *GAPDH* gene coding for a stable message was inserted in-frame and downstream of the 87 nt region, the resulting message decayed rapidly with a half-life comparable to BBB+mCRD (Figure 3, BBBspc+cd87). In contrast, the *GAPDH* sequence alone had no destabilizing effect (Figure 3, BBBspc). To rule out a nonspecific positional effect of destabilization by the 87 nt element, an irrelevant sequence from the 3′ portion of the mCRD with a similar size (92 nt) was tested (Figure 3, BBBspc+cd92). The resulting message was stable. Taken together, these experiments identified the 5′ 87 nt purine-rich sequence of the mCRD (Figure 3A, bold-faced sequence) as the minimal functional element in the 1143 nt c-*fos* coding region. Interestingly, the minimal functional element coincides with the region within the 320 nt mCRD that is recognized by at least two distinct CRD binding proteins previously detected by gel-mobility-shift and UV cross-linking assays (Chen et al., 1992).

Purification of Cytoplasmic Polypeptides Specifically Associated with the 87 nt Minimal Destabilizing Element

The above in vivo studies suggest physical contact between the mCRD and the 3′ poly(A) tail, perhaps via a bridging complex involving RNA-protein interactions. Such a complex could conceivably prevent deadenylation and RNA decay prior to translation, and translationally coupled mRNA decay might be explained by ribosome transit causing disruption of the bridging complex. This concept of a bridging complex involves proteins which bind to the poly(A) tail and to the mCRD, as well as proteins that link mCRD binding proteins to the poly(A)/PABP complex. To examine this hypothesis, we set out to purify participating protein factors. First, HeLa cells were evaluated as a source for purification of the relevant human proteins due to difficulties in growing sufficient quantities of adherent NIH 3T3 cells for large scale protein purification. UV cross-linking experiments (Figure 4A, lanes 4 and 5) showed that the two cell extracts exhibited nearly identical patterns. Therefore, we proceeded with purification of mCRD binding protein using a HeLa cytoplasmic extract.

We employed a single-step biotin/streptavidin RNA-affinity purification scheme (Yeakley et al., 1996), using a specific ribo-oligonucleotide spanning the first 24 nt purine sequence corresponding to the longest purine stretch in the 87 nt minimal element (Figure 3A, underlined sequence). Previously, we showed that this 24 nt purine sequence alone was able to associate with all the cytoplasmic RNP complexes detected in NIH 3T3 cells (Chen et al., 1992). As a negative control, a biotinyl-

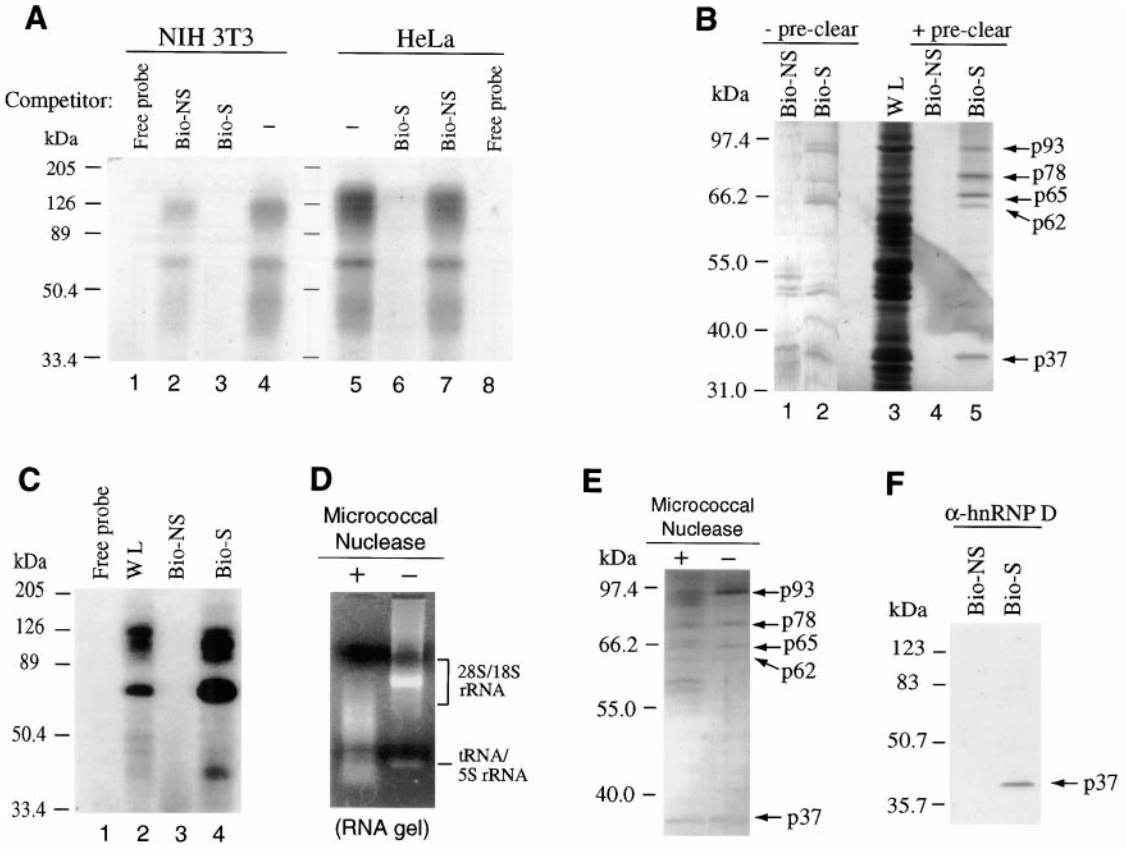

Figure 4. Identification and Purification of Proteins Interacting with the c-*fos* mCRD

(A) Cytoplasmic extracts of NIH 3T3 cells and HeLa cells exhibit similar UV cross-linked patterns. The uniformly ^{32}P-labeled RNA probe spanning the 320 nt c-*fos* mCRD was incubated at room temperature in a crude cytoplasmic lysate of NIH 3T3 cells (lanes 2 to 4) or HeLa cells (lanes 5 to 7) in the absence (lanes 4 and 5) or in the presence of 600-fold molar excess of either nonspecific biotinylated RNA competitor (Bio-NS; lanes 2 and 7) or specific biotinylated RNA corresponding to the 5′ 24 nt purine sequence of the 87 nt c-*fos* mCRD (Bio-S; lanes 3 and 6). The binding mixtures were UV irradiated prior to SDS-PAGE (7.5%–15%).

(B) SDS-PAGE and silver staining analysis of the isolated proteins. The biotinylated specific RNA (Bio-S; lanes 2 and 5) and the nonspecific control RNA (Bio-NS; lanes 1 and 4) were used in parallel runs for purification. The HeLa cytoplasmic lysates were preincubated without (−preclear, lanes 1 and 2) or with (+preclear) streptavidin agarose beads prior to affinity purification using the specific Bio-S RNA. An aliquot of isolated proteins was resolved on a denaturing SDS-9% polyacrylamide gel and analyzed by silver staining. WL: whole HeLa cytoplasmic lysate (lane 3). Purified proteins were named according to their molecular weights as shown on the right.

(C) The isolated proteins retained all the mCRD binding activities. ^{32}P-labeled RNA probe corresponding to the mCRD (lane 1) was incubated with the whole HeLa cytoplasmic lysate (lane 2) or with the proteins purified by nonspecific biotinylated RNA probe (Bio-NS; lane 3) or by specific biotinylated 24 nt purine RNA probe (Bio-S; lane 4). The binding mixtures were UV irradiated prior to SDS-PAGE (9%).

(D) RNA gel showing efficient digestion by micrococcal nuclease of cellular RNAs in the HeLa cytoplasmic lysate.

(E) Micrococcal nuclease pretreatment of HeLa cytoplasmic lysate did not abolish copurification of the five proteins isolated by the specific Bio-S probe. Proteins purified from treated or nontreated samples were analyzed by SDS-PAGE (9%).

(F) Immunoblot analysis of proteins purified by biotinylated specific (Bio-S) or nonspecific (Bio-NS) RNAs was carried out using a polyclonal antibody against hnRNP D.

ated nonspecific RNA corresponding to the β-globin coding region was also synthesized. Competition experiments showed that the unlabeled 24 nt biotinylated RNA probe, but not the nonspecific one, efficiently suppressed formation of RNP complexes (Figure 4A, lanes 2, 3, 6, and 7), demonstrating the feasibility of using the 5′-biotinylated 24 nt purine sequence for purification.

We then purified mCRD binding proteins from the HeLa cytoplasmic extract (Figure 4B). We included one extra step to further reduce nonspecific protein binding: preincubating the cytoplasmic extracts with streptavidin agarose beads prior to the RNA-affinity chromatography (Figure 4B, compare lanes 1 and 2 with lanes 4 and 5). Five well-separated bands of 37, 62, 65, 78, and 93 kDa were isolated with the specific RNA and not with the nonspecific RNA (Figure 4B, lanes 4 and 5). UV cross-linking experiments revealed nearly identical patterns of cross-linked proteins between the purified cytoplasmic proteins and the crude cytoplasmic extract of HeLa cells (Figure 4C, lanes 2 and 4), demonstrating that all the mCRD binding activities in the crude cytoplasmic lysate were purified. To further show that this group of proteins were copurified because of their specific association with the 24 nt purine sequence and not due to nonspecific RNA tethering, the RNA-affinity chromatography was repeated using lysate pretreated with micrococcal nuclease to destroy cellular RNAs as indicated by degraded rRNAs (Figure 4D). This nuclease treatment had

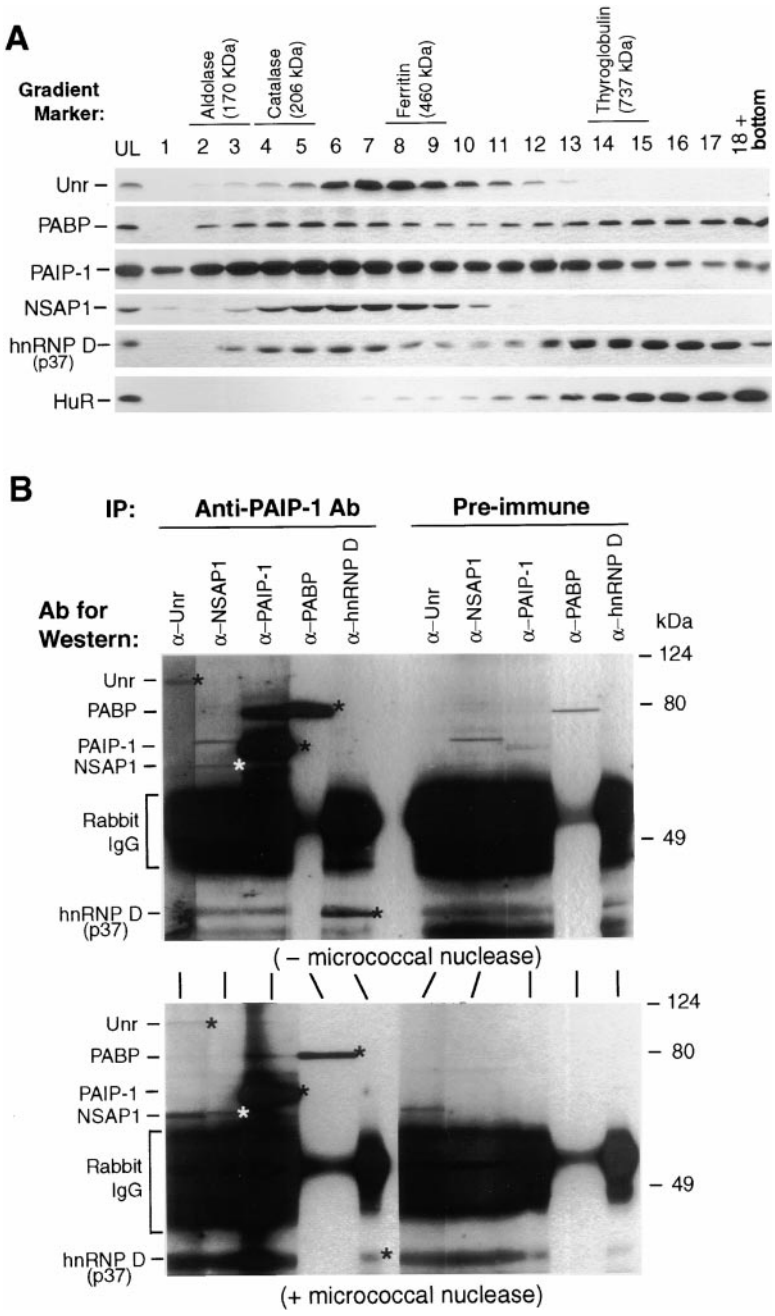

Figure 5. The Five Proteins Exist as a Complex

(A) Sucrose gradient fractionation of protein complexes. HeLa cytoplasmic lysate was fractionated on a continuous sucrose gradient (5%–20%) to resolve different protein complexes (for details, see Experimental Procedures). Protein profiles were obtained by running protein samples from each fraction (1–18 fractions) on a 9% SDS-PAGE, which was subsequently analyzed by Western blot analyses using specific antibodies. UL: unfractionated cytoplasmic lysate. Four marker proteins (Amersham-Pharmacia) were resolved through the sucrose gradient in a parallel fractionation. Peak distributions of each marker protein and its molecular mass are as depicted above protein profiles.

(B) Coimmunoprecipitation. HeLa cytoplasmic lysate with (+) or without (−) micrococcal nuclease treatment was first incubated with the rabbit anti-PAIP1 serum or preimmune serum. Antibody-antigen complexes were absorbed by protein G Sepharose beads. Precipitated antigen proteins were resolved by SDS-PAGE (9%) followed by Western blot analyses using specific antibodies as depicted above each lane. IP: immunoprecipitation. "*" marks the target protein bands.

little effect on copurification of the five proteins (see Figure 4E).

Characterization of the mCRD-Associated Proteins

The p62, p65, p78, and p93 bands were individually subjected to amino acid sequencing. The p78 band sequences corresponded to cytoplasmic poly(A) binding protein (PABP) (Görlach et al., 1994). The p65 band sequences identified it as PABP-interacting protein 1 (PAIP-1), a recently identified protein that simultaneously interacts with PABP and eIF4A (Craig et al., 1998). The other two bands, p93 and p62, had sequences corresponding to recently cloned RNA binding proteins known as Unr (Jacquemin-Sablon et al., 1994; Hunt et al., 1999) and NSAP1 (Harris et al., 1999), respectively. Unr exhibits avid binding to purine-rich sequences and is an atypical member of the cold-shock family (Triqueneaux et al., 1999). It has been reported that Unr plays a role in the internal initiation of translation of human rhinovirus RNA (Hunt et al., 1999). NSAP1 was previously isolated in a yeast two-hybrid screen through its association with a nonstructural parvovirus protein (NS1) (Harris et al., 1999). While the function for NSAP1 is unknown, it displays 80% sequence homology with heterogeneous nuclear ribonucleoprotein R (hnRNP R) (Hassfeld et al., 1998). hnRNP R contains three RNA-recognition motifs (RRM) with well-conserved RNP-1 and RNP-2 submotifs. In addition, the C terminus of the protein

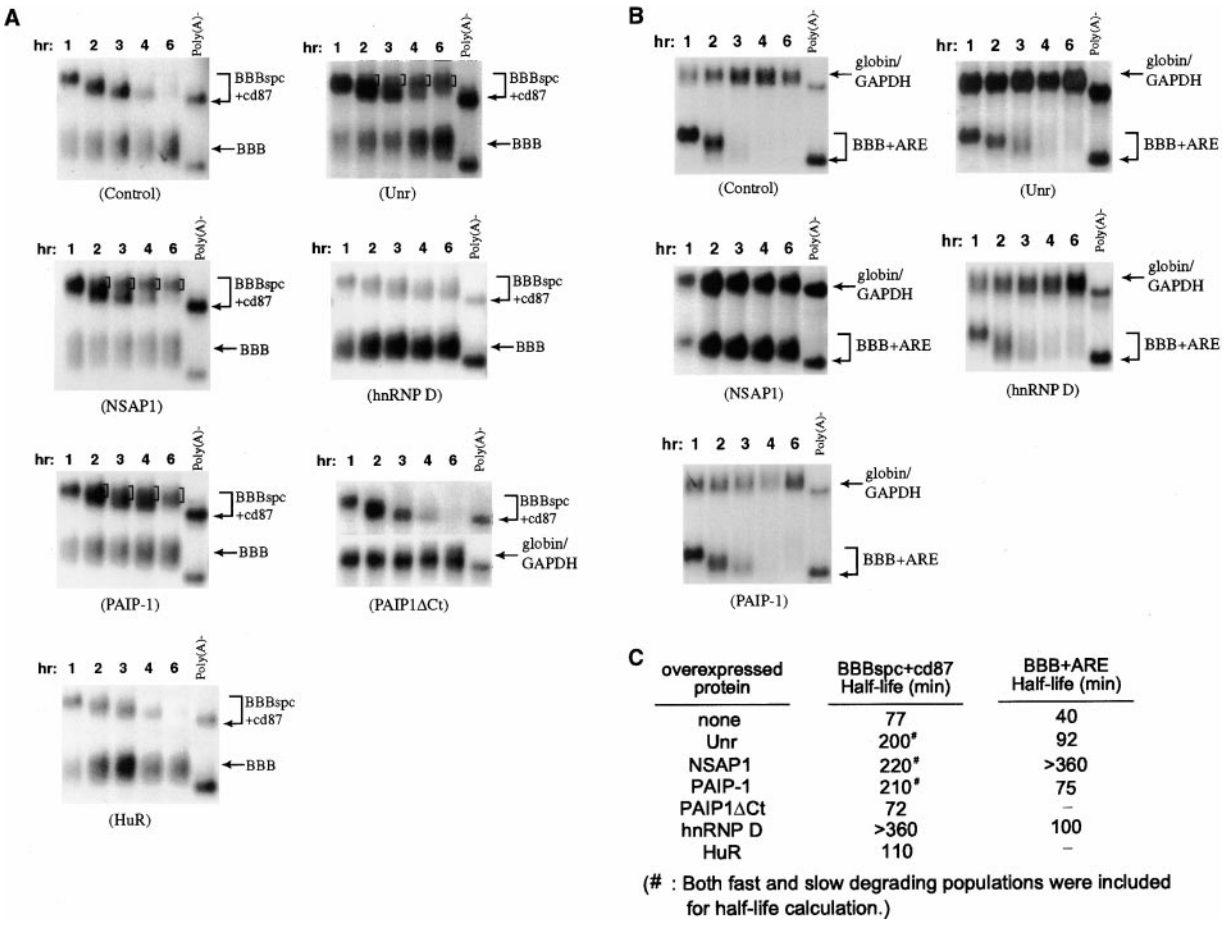

Figure 6. Ectopic Expression of the c-*fos* mCRD-Associated Proteins Results in RNA Stabilization by Impeding Deadenylation

Northern blots showing deadenylation and decay of BBBspc+cd87 (A) or BBB+ARE (B) in the absence (control) or presence of ectopically expressed Unr, NSAP1, PAIP1, hnRNP D/p37, PAIP1ΔCt, or HuR. Slow degrading populations of BBBspc+cd87 mRNA were bracketed in the blots showing RNA decay under overexpression of Unr, NSAP1, and PAIP-1. (C) Summary of the half-lives of the reporter mRNA in the absence or presence of various ectopically expressed proteins as shown in panels (A) and (B). Transient transfection of NIH 3T3 cells, RNA isolation, time course experiments, and RNA blot analysis were carried out as described in the legend to Figure 1.

contains an arginine/glycine-rich domain (RGG box) known for its collaboration with RRMs for RNA recognition and binding specificity; it is also involved in the protein/protein interactions (Dreyfuss et al., 1993). The identities of the four proteins were individually confirmed by Western blot analysis of the purified proteins using specific antibodies (data not shown). Although insufficient protein was available for peptide sequencing, the p37 band was recognized by antibody raised against the hnRNP D (Figure 4F). The immunoblot evidence strongly suggests that our p37 is the p37 isoform of hnRNP D.

Unr, PABP, PAIP1, NSAP1, and hnRNP D Form a Complex Assembled on the mCRD

Given that only Unr has been shown to have strong and specific affinity for purine-rich sequence and that the five proteins were copurified at relatively high ionic strength, it was possible that these proteins copurified as a complex via Unr's interaction with the 24 nt purine substrate. Two complementary lines of experiments were carried out to address this possibility. First, sucrose-gradient fractionations of the HeLa cytoplasmic extract were analyzed by Western blotting. The results (Figure 5A) showed that a significant portion of all five proteins comigrated in the upper part of the gradient (fractions 5–7). In contrast, HuR, which was shown previously to have no effect on mCRD-mediated decay (Peng et al., 1998), only appeared in the bottom half of the gradient. These experiments suggested that the five proteins exist as a complex in vivo. Since these proteins may have other cellular functions in the cytoplasm, a slight shift of peak fractions between Unr and other proteins may thus indicate their involvement in the formation of other subcomplexes.

Second, we did coimmunoprecipitation experiments. HeLa cytoplasmic extract was first incubated with antibody against PAIP-1. The immunoprecipitate was then analyzed for the existence of other proteins by Western blot analysis. The results (Figure 5B, upper panel) showed that all five proteins are coprecipitated by anti-PAIP-1 antibody and not by preimmune serum. To rule out the possibility that coprecipitation of these proteins by anti-PAIP-1 antibody is due to their association with

RNA and not due to protein/protein interactions, the experiment was repeated using the lysate pretreated with micrococcal nuclease. RNA gel confirmed the complete degradation of RNAs after micrococcal nuclease treatment (data not shown). The results (Figure 5B, lower panel) showed that all five proteins can still be coimmunoprecipitated. Taken together, these two independent lines of evidence support that these proteins form a multiprotein complex.

Ectopic Expression of mCRD-Associated Proteins Stabilizes RNA by Impeding Deadenylation

Rapid deadenylation directed by the mCRD is coupled to translation (Shyu et al., 1991; Schiavi et al., 1994). What is the molecular mechanism underlying this translational dependence? Our data described so far are consistent with the idea that a multiprotein complex bridges the mCRD and the 3′ poly(A) tail, which could then prevent deadenylation prior to translation initiation. Following translation initiation, this interaction is interrupted or modified, thereby leading to rapid deadenylation. This model predicts that interfering with the formation of the bridging complex prior to translation initiation would stabilize mRNA by specifically impeding deadenylation.

To test this model, we overexpressed candidate *trans*-acting factors as an attempt to interfere with the proper stoichiometry for proteins in the complex and thus its bridging function. The results showed that ectopic expression of these proteins individually resulted in significant stabilization of the BBBspc+cd87 mRNA (Figure 6). It was striking that with overexpression of Unr, PAIP-1, or NSAP-1 a subpopulation of reporter message showed no deadenylation (Figure 6, see bracketed bands) while the remaining population underwent normal deadenylation and decay. Ectopic expression of hnRNP D/p37 had significant retarding effect on poly(A) shortening of the entire reporter mRNA population. In contrast, ectopic expression of HuR, an ARE binding protein, or of a mutant PAIP-1 whose interaction with PABP is dramatically reduced (PAIP1ΔCT), had little effect on deadenylation or decay of reporter mRNA (Figure 6A).

To test whether ectopic expression of these proteins affects other classes of RNA destabilizing element, we also examined the decay of β-globin mRNA bearing an ARE (BBB+ARE). The results showed that overexpression of Unr, PAIP1, and hnRNP D individually had a modest stabilization effect, whereas overexpression of NSAP1 caused profound stabilization of BBB+ARE message by blocking the deadenylation of BBB+ARE message (Figure 6B). The expression of the corresponding proteins in the cytoplasm in the above experiments was confirmed by Western blot analysis (data not shown). Taken together, these results support a role for Unr, PAIP1, NSAP1, and hnRNP D in the decay mediated by the mCRD. They also suggest that NSAP1 may be a common factor recruited by different destabilizing elements for directing the deadenylation.

Discussion

The following critical observations must be taken into account when explaining how the c-*fos* mCRD exerts its potent destabilizing function. First, the mCRD directs accelerated deadenylation, which precedes degradation of the RNA body (Shyu et al., 1991; Schiavi et al., 1994). Second, the mCRD is recognized as a signal in the mRNA sequence or structure per se and ribosome transit is required to activate this signal (Wellington et al., 1993). Third, the mCRD must be some distance away from the poly(A) tail in the mRNA sequence for the mCRD to function (this study). In addition, five proteins including the PABP and the purine-rich sequence binding protein, Unr, that associate specifically with the mCRD are able to form a complex (this study). Given these observations, we propose a model involving direct interaction between the mCRD and the 3′ poly(A) tail via a bridging complex consisting of the five proteins. Before the mCRD containing mRNA is translated, the bridging complex may prevent deadenylation by stabilizing the poly(A) tail/PABP complex, thus blocking poly(A) nuclease access to the poly(A) tail. During translation, ribosomal movement up to or across the mCRD displaces or reorganizes the bridging complex, thereby allowing formation of metastable structures which expose the poly(A) tail to nuclease attack, e.g., by stripping PABP off the poly(A) tail. This could also explain why blocking translation by a targeted hairpin insertion near the cap site stabilizes an mRNA containing the mCRD (Schiavi et al., 1994; Chen et al., 1995).

A recent in vitro study (Gao et al., 2000), showing that both 5′ cap and 3′ poly(A) are required for recruiting a poly(A) nuclease, DAN (Körner and Wahle, 1997), to degrade poly(A) tail from in vitro RNA substrate, suggests another possibility. The mCRD may outcompete the 5′ cap to interact with 3′ poly(A) tail. This in turn prevents efficient recruitment of DAN. Thus, requirement for translation could be explained if DAN is recruited only when the 5′ cap and 3′ poly(A) interaction is restored following disruption of the bridging complex as a result of ribosome transit. Or, there exists a three-way interaction between 5′ cap, 3′ poly(A), and the mCRD, which prevents efficient recruitment of DAN. As ribosomes traverse through the mCRD, the interaction between mCRD and 5′ cap/3′ poly(A) tail is disrupted and/or modified, leading to rapid deadenylation by DAN. We propose that the formation of the mRNP structure involving the mCRD and the poly(A) tail prior to translation initiation is a prerequisite for the mCRD-mediated decay, and constitutes an early event that commits the mCRD-bearing mRNA to later deadenylation and decay in a translation-dependent manner.

Why is a minimal distance of ~450 nt spacer between the mCRD and the poly(A) tail required? Since RNA typically forms secondary or tertiary structures and since RNA is also coated with RNA binding proteins, one possibility is that these RNA/RNA and RNA/protein interactions may impose physical constraints on the spacer. This in turn limits the proper interactions between the mCRD and the poly(A) tail or the cap/poly(A) tail. On the other hand, it is also possible that such a "long" minimal spacer may prevent efficient interaction of these two RNA entities. Future experiments involving in vitro reconstitution or electron microscopy may shed light on this interesting issue.

Several lines of evidence we reported here support the existence of the multiprotein bridging complex (see Figures 4 and 5). The RNA binding specificities and colo-

calization of the five proteins suggest the following characteristics of the bridging complex between the mCRD and the poly(A) tail. When the complex forms, PABP is associated with the poly(A) tail and the Unr protein binds to the purine stretches in the mCRD. It is possible that PAIP-1, NSAP-1, and hnRNP D interact with one another to form a central core of the bridging complex that associates with poly(A)/PABP through PAIP1. The identification of Unr known to be involved in internal translation initiation (Hunt et al., 1999) in the bridging complex for mCRD-mediated decay has an important mechanistic implication. Formation of the bridging complex may prevent proper interaction between the 5′ cap and the 3′ poly(A) for translation initiation. Recruitment of Unr in the bridging complex may thus enhance translation initiation in a cap-independent manner. Our results also provide a clue about one real role for PAIP-1, a variation of the "conventional" initiation factor function. For example, it may be part of a decay complex which tightly couples translation and mRNA decay.

A few possibilities that are not mutually exclusive may be envisaged to explain retardation of deadenylation and stabilization of the reporter message by overexpressing NSAP1, PAIP-1, or hnRNP D/p37. First, overexpression of the proteins may result in the formation of an aberrant bridging complex or disrupt formation of the complex. Second, the effect could be due to titration by these proteins of a factor required for poly(A) shortening. Third, translation initiation may be inhibited as a result of overexpression of these proteins, leading to loss of rapid deadenylation and consequent RNA stabilization. Nevertheless, the ability of these proteins to interfere with the deadenylation step is consistent with our model that deadenylation is a necessary first step in message decay. However, our data do not rule out other possibilities. For example, PABP or PABP/poly(A) complex may directly interact with the mCRD without involving a bridging complex. Also, the RNA stabilizing effect exerted by ectopically expressed NSAP1, PAIP-1, hnRNP D, and Unr may be due to their direct binding to the mCRD. Thus, these proteins may function as a negative regulator in mCRD-mediated mRNA turnover.

It is particularly intriguing to find that hnRNP D and NSAP1 are involved in mRNA decay directed by distinct RNA turnover determinants, namely, the AU-rich element, and the c-*fos* mCRD (Loflin et al., 1999 and this study). It suggests that RNA turnover determinants residing in different parts of the message may have evolved distinct ways to recruit common factors, e.g., hnRNP D and NSAP1, as well as determinant-specific factors for eliciting communication with the poly(A) tail. This communication between each mRNA stability determinant and the poly(A) tail then sets up a distinct mRNP structure that influences the balance between translation and deadenylation/decay in the process of producing the final protein product.

How general is the c-*fos* mCRD-mediated decay mechanism? c-*fos* is a member of a large class of early-response genes (ERGs), whose coordinated and transient expression accompanies the transition of cells from the resting state, G_0, into the cell cycle (Herschman, 1991). A common feature of ERG mRNAs is that their stability is profoundly increased when translation is blocked (Greenberg and Belasco, 1993). Decay mediated by protein-coding determinants in c-*fos* points to the possibility that coupling of mRNA decay to translation is a general theme among ERG transcripts. In this regard, another example of a destabilizing sequence in the protein-coding region is found in mammalian c-*myc* mRNA, another ERG mRNA (Laird-Offringa, 1991; Wisdom and Lee, 1991; Herrick and Ross, 1994). Interestingly, the c-*myc* protein-coding determinant targets c-*myc* mRNA for accelerated deadenylation and turnover in a translation-dependent manner, similar the to c-*fos* coding determinants (Wisdom and Lee, 1991; Herrick and Ross, 1994).

Our experiments have revealed a novel role for the 3′ poly(A) tail which provides mechanistic insights into several fundamental issues concerning translation and RNA turnover. First, a dynamic interaction between the transcribed portion of a message and its poly(A) tail clearly exists to influence the rate of deadenylation. Second, the 3′ poly(A) tail plays an active role, instead of a passive and protective role as previously thought, in the mRNA decay. Third, the evidence that the bridging complex contains RNA binding proteins that can or have the potential to shuttle between the nucleus and cytoplasm supports the concept that shuttling RNA binding proteins have not only nuclear but also cytoplasmic functions (Shyu and Wilkinson, 2000). All of these point to functional interconnection between posttranscriptional events in the nucleus and in the cytoplasm. As translationally coupled decay may be a general feature among a large group of labile transcripts whose transient existence in the cytoplasm is induced by growth factors, neural transmitters, cytokines, immune response, and cellular stresses, further characterization of the structure and dynamics of the bridging complex operating in the c-*fos* mCRD may unravel important new mechanisms of control of cell growth and differentiation.

Experimental Procedures

Plasmid Construction

When necessary, DNA with 5′- or 3′-protuding ends was treated with Klenow fragment or T4 DNA polymerase to make the ends blunt. When convenient restriction sites were not available for cloning, standard polymerase chain reaction (PCR) techniques were employed to amplify desired sequences of the c-*fos* coding region using pBFB as the template. Plasmids pBBB, pBBB4, pBFB, pBBB+ARE, pSVB10, pSVα/GAPDH, pSV-mAUF1/p37, pcDNA3-PAIP1, and pcDNA3-PAIP1ΔCt were constructed as described previously (Shyu et al., 1989, 1991; Chen and Shyu, 1994; Chen et al., 1995; Craig et al., 1998; Loflin et al., 1999).

To generate pBBB+mCRD, an EcoRV-StuI fragment encoding the 320 nt mCRD of human c-*fos* mRNA (spanning 391–709 nt downstream from the AUG codon) was inserted in-frame between the *Acc*I (blunt ended) and NcoI (blunt ended) sites in the second exon of the rabbit β-globin gene in pBBB (Shyu et al., 1989). Plasmid pBBBspc was constructed by inserting a 316 bp MscI-EagI (blunt ended) fragment spanning nucleotides 476 to 792 of the rat glyceraldehyde 3′-phosphate dehydrogenase cDNA (Fort et al., 1985) into the BamHI (blunt ended) site of pBBB. The fragment containing the 87 nt 5′ region or the 92 nt 3′ portion of the 320 nt mCRD was inserted in-frame into pBBB or pBBBspc (between the AccI and NcoI sites which had been blunt ended) to generate pBBB+cd87, pBBB+cd92, pBBBspc+cd87, or pBBBspc+cd92, respectively.

When necessary, an XbaI linker (New England BioLab) containing stop codons in all three reading frames was used to stop translation in hybrid constructs described below. Plasmid pBFBΔC1 was constructed by replacing the StuI-BglII (blunt ended) fragment spanning

the c-*fos* coding region downstream of the 320 nt mCRD in pBFB (Shyu et al., 1989) with the XbaI linker. To generate pFBxcd1, the NcoI (blunt ended)-BglII fragment spanning the second exon, second intron, and part of the third exon of the rabbit β-globin gene in pBBB4 (Shyu et al., 1989) was used to replace in-frame the StuI-BglII fragment encoding the human c-*fos* carboxyl terminus in pBFB. Plasmid pFBxcd2 was constructed by replacing the MluI-StuI fragment in pBFB with the MluI-BamHI(blunt ended) fragment from pBBB4. Plasmid pBFBΔC2 was constructed by deleting the 290 bp StuI-PvuII fragment in pBFB, which spans an internal segment of Fos carboxyl terminus. The same approach was used for the construction of pBFBΔC3 except that a 269 bp StuI-PspEI (blunt ended) fragment in pBFB was deleted and the resulting plasmid was fused in-frame. To generate pBFBΔC4, the PspEI-BglII (blunt ended) fragment in pBFB, spanning the very 3′ portion of the c-*fos* coding region, was replaced with the XbaI linker. Plasmid pFBxcd3 was constructed by replacing the 1.4 kb MluI-PaeI (blunt ended) fragment in pBFB with the 0.6 kb MluI-HindII fragment from pBBB4. To generate pBBB+mCRDΔC, the StuI-BglII (blunt ended) fragment spanning the c-*fos* coding region immediately downstream of the 320 nt mCRD in pFBxcd3 was replaced with the XbaI linker. The XbaI linker was inserted into the StuI site of pFBxcd3 to create pFBxcd4. To construct pFBxcd5, the StuI-BglII (blunt ended) fragment in pFBxcd3 was replaced with an inverted sequence carrying a stop codon at its 5′ end.

To create the plasmid pSV-mNSAP1, a 1.7 kb fragment spanning the NSAP1 coding region was amplified from a human placental cDNA library (Clontech) by PCR using the following primers: sense 5′-TCTGGTCGACATGGCTACAGAACATGTTAATG-3′ and antisense 5′-GCTCTAGATCTTCATTGTAACAGGTCAGG-3′. The 1.7 kb fragment was digested with AccI and XbaI and then inserted between the AccI and XbaI sites of pMyc-ovep (Loflin et al., 1999). DNA sequencing was performed to confirm the NSAP1 cDNA and the pSV-mNSAP1 construct. The plasmid pSG-UNRFlag for ectopic expression of Unr in mammalian cells was provided by H. J.- S.

Cell Culture, DNA Transfection, Northern Analysis, and Cell Extract Preparation

Culturing, transient transfection, and serum stimulation of mouse NIH 3T3 cells were performed as described previously (Shyu et al., 1989). Isolation of total cytoplasmic RNA and Northern blot analysis were conducted as described previously (Shyu et al., 1996). The quantitation of data was obtained by scanning the radioactive blots with an imager (Packard). The preparation of cytoplasmic lysate from NIH 3T3 cells has been described previously (Peng et al., 1998). Culturing and preparation of cytoplasmic lysates from human HeLa cells were performed as described previously (Zapp and Berget, 1989) with a few changes. Briefly, cytoplasmic lysates were prepared from HeLa cells by lysis at 4°C in a hypotonic lysis/extraction buffer containing 10 mM HEPES (pH 7.9), 1.5 mM $MgCl_2$, 10 mM KCl, 0.5 mM dithiothreitol (DTT), 5 μg/ml of aprotinin, 10 μg/ml of leupeptin, 1 μg/ml of Pepstatin A, and 100 μg/ml PMSF. Nuclei were removed by centrifugation (2000 × g) at 4°C for 15 min. Protein concentration was analyzed by the BCA protein assay reagent according to the manufacturer's protocol (Pierce).

Analysis of RNP Interactions

RNA probes synthesized and binding reactions performed in vitro were as described previously (Chen et al., 1992) with minor modifications. The final volume for binding reaction was 10 μl. Cytoplasmic lysate (5 μg of protein, about 1.4–1.7 × 10^4 equivalent of cells) and ^{32}P-labeled RNA (1 ng) were incubated at room temperature for 15 min. Subsequently, unbound RNA was digested for 20 min by RNase A (500 μg/ml final) at room temperature. RNP complexes were resolved in nondenaturing low-ionic-strength 6% polyacrylamide gels. UV cross-linking experiments were carried out as described previously (Chen et al., 1992).

Streptavidin-Biotin RNA-Affinity Chromatography

Control biotinylated RNA (nonspecific biotinylated RNA probe, 5′-AGGGAGAGACAAGCUUGCAUGCCUGCAGGUC-3′) was transcribed with equal amounts of biotin-14-CTP (Gibco BRL) and CTP to ensure incorporation of three to four biotin molecules per transcript. Transcription reactions were performed according to the instructions of Promega. The 5′ end-biotinylated specific RNA probe (specific biotinylated RNA probe [Bio-S], 5′-CCAGAAGAAGAAGA GAAAAGGAGAA-3′) containing the 24 nt purine sequence from c-*fos* mCRD was synthesized by CyberSyn (Lenni, PA).

Purification of the proteins was performed as described below. Protein extracts were first precleared by incubating 200 mg of cytoplasmic proteins from HeLa cells with 3 ml of a slurry 50% preblocked streptavidin-coated agarose beads (Sigma), for 3 hr at 4°C in 50 ml Binding Buffer (10 mM Hepes [7.6], 3 mM $MgCl_2$, 5 mM EDTA [8.0], 2 mM DTT, 5% Glycerol, 0.5% NP-40, 3 mg/ml Heparin, and 0.5 mg/ml Yeast RNA) supplemented with 40 mM KCl and RNasin (0.3 U/μl, final). Beads were pelleted and the supernatant was incubated with 600 μg biotinylated-RNA probe as described above for 2 hr. The binding mixture was then incubated with 3 ml of the 50% slurry preblocked streptavidin-coated agarose beads for 2 hr. Beads were pelleted and washed three times in Binding Buffer with 40 mM KCl and twice in Binding Buffer with 300 mM KCl. Isolated proteins were eluted from the beads by incubating with Elution Buffer (10 mM Hepes [7.6], 3 mM $MgCl_2$, 5 mM EDTA, 2 mM DTT, 0.2% glycerol, and 2 M KCl) for 20 min at 4°C. Protein microsequencing was performed using the core facilities at Baylor College of Medicine. When necessary, whole cytoplasmic lysate from HeLa cells was incubated in the presence of micrococcal nuclease (10 U/ml final concentration) (Gibco-BRL) at 37°C for 30 min.

Sucrose Gradient Fractionation

Sucrose gradient fractionation was performed as previously described for polysome profile analysis (Chen et al., 1995). 8 mg of HeLa cytoplasmic lysate was layered on the top of a continuous sucrose gradient (5%–20% sucrose in 10 mM Tris-HCl [pH 7.5], 140 mM NaCl, 1.5 mM $MgCl_2$). The gradient was centrifuged at 35,000 rpm for 5 hr at 4°C in a Beckman SW41 swing bucket rotor. Eighteen 0.5 ml fractions were collected after centrifugation. Protein samples were analyzed by running an aliquot of each fraction on 9% SDS-PAGE followed by Western blot analyses. Specific antibodies were used to detect the localization of candidate proteins as described below. Protein size markers (Amersham-Pharmacia) were also included in the parallel run.

Antibodies, Western Blot Analysis, and Coimmunoprecipitation

Western blot analyses were carried out using ECL kit (Amersham). The blots were probed with specific antibodies as described in the figure legends. The mAb against the human PABP (10E10; mouse IgG) was kindly provided by G. Dreyfuss. The rabbit polyclonal antibody against the human NSAP1 was kindly provided by C. Astell. The rabbit polyclonal antibody against the C-terminal domain of hnRNP D was kindly provided by N. Maizels. The polyclonal antibody against the Unr was raised in rabbit by injecting purified Unr proteins. The anti-HuR mAb (mouse IgG) was kindly provided by J. A. Steitz. The rabbit polyclonal antibody against the PAIP1 was as described previously (Craig et al., 1998).

Coimmunoprecipitation reactions were performed with anti-PAIP1 or preimmune serum (Craig et al., 1998). The HeLa cytoplasmic lysates with or without micrococcal nuclease treatment were precleared with protein G Sepharose beads (Amersham-Pharmacia) and then subjected to immunoprecipitation at 4°C with antibodies. Immunoprecipitates were directly resuspended in SDS loading buffer, run on SDS-PAGE (9%), and analyzed by Western blot analyses using specific antibodies as described in the legend to Figure 5.

Acknowledgments

We thank R. Kulmacz, R. Lloyd, and M. Wilkinson for critical reading of the manuscript and their valuable comments; P. Carpenter for advice on RNA-affinity chromatography; R. Cook for his wonderful work concerning the microsequencing of the purified proteins; C.-T. Chang for technical assistance; N. Maizels for the hnRNP D antibody; C. Astell for the NSAP1 antibody; J. A. Steitz for the HuR mAb; and G. Dreyfuss for the PABP antibody. Special thanks go to

S. Berget and her lab members for generously providing us with HeLa cytoplasmic extracts. This work was supported initially by a grant from National Institutes of Health (GM 46454) and later by an NIH grant (GM 59211). A.-B. S. was the recipient of an American Heart Association Established Investigator Award.

Received May 5, 2000; revised August 11, 2000

References

Caruccio, N., and Ross, J. (1994). Purification of a human polyribosome-associated 3′ to 5′ exoribonuclease. J. Biol. Chem. *269*, 31814–31821.

Chen, C.Y., and Shyu, A.B. (1994). Selective degradation of early-response-gene mRNAs: functional analyses of sequence features of the AU-rich elements. Mol. Cell. Biol. *14*, 8471–8482.

Chen, A.C.-Y., and Shyu, A.-B. (1995). AU-rich elements: characterization and importance in mRNA degradation. Trends Biochem. Sci. *20*, 465–470.

Chen, C.Y., You, Y., and Shyu, A.B. (1992). Two cellular proteins bind specifically to a purine-rich sequence necessary for the destabilization function of a c-fos protein-coding region determinant of mRNA instability. Mol. Cell. Biol. *12*, 5748–5757.

Chen, C.Y., Chen, T.M., and Shyu, A.B. (1994). Interplay of two functionally and structurally distinct domains of the c-fos AU-rich element specifies its mRNA-destabilizing function. Mol. Cell. Biol. *14*, 416–426.

Chen, C.Y., Xu, N., and Shyu, A.B. (1995). mRNA decay mediated by two distinct AU-rich elements from c-fos and granulocyte-macrophage colony-stimulating factor transcripts: different deadenylation kinetics and uncoupling from translation. Mol. Cell. Biol. *15*, 5777–5788.

Craig, A.W., Haghighat, A., Yu, A.T., and Sonenberg, N. (1998). Interaction of polyadenylate-binding protein with the eIF4G homologue PAIP enhances translation. Nature *392*, 520–523.

Dreyfuss, G., Matunis, M.J., Pinol-Roma, S., and Burd, C.G. (1993). hnRNP proteins and the biogenesis of mRNA. Annu. Rev. Biochem. *62*, 289–321.

Fort, P., Marty, L., Piechaczyk, M., Sabrouty, S.E., Dani, C., Jeanteur, P., and Blanchard, J.M. (1985). Various rat adult tissues express only one major mRNA species from the glyceraldehyde-3-phosphate-dehydrogenase multigenic family. Nucleic Acids Res. *13*, 1431–1442.

Gallie, D.R. (1991). The cap and poly(A) tail function synergistically to regulate mRNA translational efficiency. Genes Dev. *5*, 2108–2116.

Gao, M., Fritz, D.T., Ford, L.P., and Wilusz, J. (2000). Interaction between a poly(A)-specific ribonuclease and the 5′ cap influences mRNA deadenylation rates in vitro. Mol. Cell *5*, 479–488.

Görlach, M., Burd, C.G., and Dreyfuss, G. (1994). The mRNA poly(A)-binding protein: localization, abundance, and RNA-binding specificity. Exp. Cell Res. *211*, 400–407.

Greenberg, M.E., and Belasco, J.G. (1993). Control of the decay of labile protooncogene and cytokine mRNAs. In Control of Messenger RNA Stability, J.G. Belasco and G. Brawerman, eds. (San Diego, CA: Academic Press), pp. 199–218.

Harris, C.E., Boden, R.A., and Astell, C.R. (1999). A novel heterogeneous nuclear ribonucleoprotein-like protein interacts with NS1 of the minute virus of mice. J. Virol. *73*, 72–80.

Hassfeld, W.C.E., Mathison, D.A., Portman, D., Dreyfuss, G., Steiner, G., Tan, E.M. (1998). Molecular definition of heterogeneous nuclear ribonucleoprotein R (hnRNP R) using autoimmune antibody: immunological relationship with hnRNP P. Nucleic Acids Res. *26*, 439–445.

Hentze, M.W., and Kulozik, A.E. (1999). A perfect message: RNA surveillance and nonsense-mediated decay. Cell *96*, 307–310.

Herrick, D.J., and Ross, J. (1994). The half-life of c-myc mRNA in growing and serum-stimulated cells: influence of the coding and 3′ untranslated regions and role of ribosome translocation. Mol. Cell. Biol. *14*, 2119–2128.

Herschman, H.R. (1991). Primary response genes induced by growth factors and tumor promoters. Annu. Rev. Biochem. *60*, 281–319.

Hunt, S.L., Hsuan, J.J., Totty, N., and Jackson, R.J. (1999). unr, a cellular cytoplasmic RNA-binding protein with five cold-shock domains, is required for internal initiation of translation of human rhinovirus RNA. Genes Dev. *15*, 437–438.

Jacobson, A. (1996). Poly(A) metabolism and translation: The closed-loop Model. In Translational Control, J.W.B. Hershey, M.B. Mathews, and N. Sonenberg, eds. (Plainview, NY: Cold Spring Harbor Laboratory Press), pp. 451–480.

Jacquemin-Sablon, H., Triqueneaux, G., Deschamps, S., le Maire, M., Doniger, J., and Dautry, F. (1994). Nucleic acid binding and intracellular localization of unr, a protein with five cold shock domains. Nucleic Acids Res. *22*, 2643–2650.

Körner, C.G., and Wahle, E. (1997). Poly(A) tail shortening by a mammalian poly(A)-specific 3′-exoribonuclease. J. Biol. Chem. *272*, 10448–10456.

Laird-Offringa, I.A. (1991). Rapid c-myc degradation does not require (A+U)-rich sequences or complete translation of the mRNA. Nucleic Acids Res. *19*, 2387–2394.

Loflin, P.A., Chen, C.-Y. A., and Shyu, A.-B. (1999). Unraveling a cytoplasmic role for hnRNP D in the in vivo mRNA destabilization directed by the AU-rich element. Genes Dev. *13*, 1884–1897.

Manley, J.L., and Proudfoot, N.J. (1994). RNA 3′ ends: Formation and function-meeting review. Genes Dev. *8*, 259–264.

Peng, S.-P., Chen, C.-Y., Xu, N., and Shyu, A.-B. (1998). RNA stabilization by the AU-rich element binding protein, HuR, an ELAV protein. EMBO J. *17*, 3461–3470.

Preiss, T., and Hentze, M.W. (1998). Dual function of the messenger RNA cap structure in poly(A)-tail-promoted translation in yeast. Nature *392*, 516–520.

Preiss, T., and Hentze, M.W. (1999). From factors to mechanisms: translation and translational control in eukaryotes. Curr. Opin. Gene Dev. *9*, 515–521.

Ross, J. (1995). mRNA stability in mammalian cells. Microbiol. Rev. *59*, 423–450.

Sachs, A.B., Sarnow, P., and Hentze, M.W. (1997). Starting at the beginning, middle, and end: translation initiation in eukaryotes. Cell *89*, 831–838.

Schiavi, S.C., Wellington, C.L., Shyu, A.B., Chen, C.Y., Greenberg, M.E., and Belasco, J.G. (1994). Multiple elements in the c-fos protein-coding region facilitate mRNA deadenylation and decay by a mechanism coupled to translation. J. Biol. Chem. *269*, 3441–3448.

Shyu, A.-B., and Wilkinson, M.F. (2000). The double lives of shuttling mRNA binding proteins. Cell *102*, 135–138.

Shyu, A.-B., Greenberg, M.E., and Belasco, J.G. (1989). The c-fos mRNA is targeted for rapid decay by two distinct mRNA degradation pathways. Genes Dev. *3*, 60–72.

Shyu, A.-B., Belasco, J.G., and Greenberg, M.G. (1991). Two distinct destabilizing elements in the c-fos message trigger deadenylation as a first step in rapid mRNA decay. Genes Dev. *5*, 221–232.

Shyu, A.-B., Garcia-Sanz, J.A., and Mullner, E., eds. (1996). Analysis of mRNA decay in mammalian cells. (London: Academic Press).

Tarun, S.Z.J., Wells, S.E., Deardorff, J.A., and Sachs, A.B. (1997). Translation initiation factor eIF4G mediates in vitro poly(A) tail-dependent translation. Proc. Natl. Acad. Sci. USA *94*, 9046–9051.

Triqueneaux, G., Velten, M., Franzon, P., Dautry, F., and Jacquemin-Sablon, H. (1999). RNA binding specificity of Unr, a protein with five cold shock domains. Nucleic Acids Res. *27*, 1926–1934.

Wellington, C.L., Greenberg, M.E., and Belasco, J.G. (1993). The destabilizing elements in the coding region of c-fos mRNA are recognized as RNA. Mol. Cell. Biol. *13*, 5034–5042.

Wells, S.E., Hillner, P.E., Vale, R.D., and Sachs, A.B. (1998). Circularization of mRNA by eukaryotic translation initiation factors. Mol. Cell *2*, 135–140.

Wisdom, R., and Lee, W. (1991). The protein-coding region of c-myc mRNA contains a sequence that specifies rapid mRNA turnover and induction by protein sythesis inhibitors. Genes Dev. *5*, 232–243.

Yeakley, J.M., Morfin, J.P., Rosenfeld, M.G., and Fu, X.D. (1996). A complex of nuclear proteins mediates SR protein binding to a purine-rich splicing enhancer. Proc. Natl. Acad. Sci. USA *93*, 7582–7587.

Yeilding, N.M., Procopio, W.N., Rehman, M.T., and Lee, W.M. (1998). c-myc mRNA is down-regulated during myogenic differentiation by accelerated decay that depends on translation of regulatory coding elements. J. Biol. Chem. *273*, 15749–15757.

Yen, T.J., Machlin, P.S., and Cleveland, D.W. (1988). Autoregulated instability of beta-tubulin mRNAs by recognition of the nascent amino terminus of beta-tubulin. Nature *334*, 580–585.

Zapp, M.L., and Berget, S.M. (1989). Evidence for nuclear factors involved in recognition of 5′ splice sites. Nucleic Acids Res. *17*, 2655–2674.

Zhang, S., Welch, E.M., Hogan, K., Brown, A.H., Peltz, S.W., and Jacobson, A. (1997). Polysome-associated mRNAs are substrates for the nonsense-mediated mRNA decay pathway in Saccharomyces cerevisiae. RNA *3*, 234–244.